

Electronic Supplementary Information

**Defects engineered SnO₂ nanoparticles enable strong CO₂ chemisorption
toward efficient electroconversion to formate**

Baoxing Ning,^a Miaoqiao Liu,^a Yanjie Hu,^a Hao Jiang,^{a,*} Chunzhong Li^{a,b},

^a Key Laboratory for Ultrafine Materials of Ministry of Education, Frontiers Science Center for
Materiobiology and Dynamic Chemistry, School of Materials Science and Engineering, East
China University of Science & Technology, Shanghai 200237, China

Email: jianghao@ecust.edu.cn

^b Shanghai Engineering Research Center of Hierarchical Nanomaterials, School of Chemical
Engineering, East China University of Science and Technology, Shanghai 200237, China

Supporting Figures

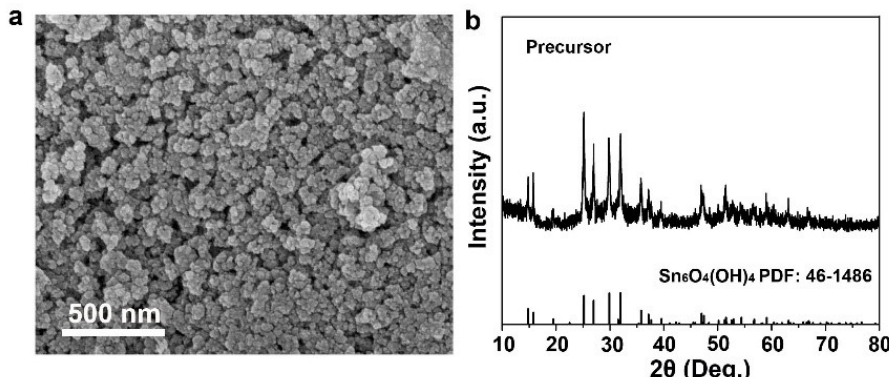


Fig. S1. (a)The SEM imagine, (b) XRD pattern of the precursor.

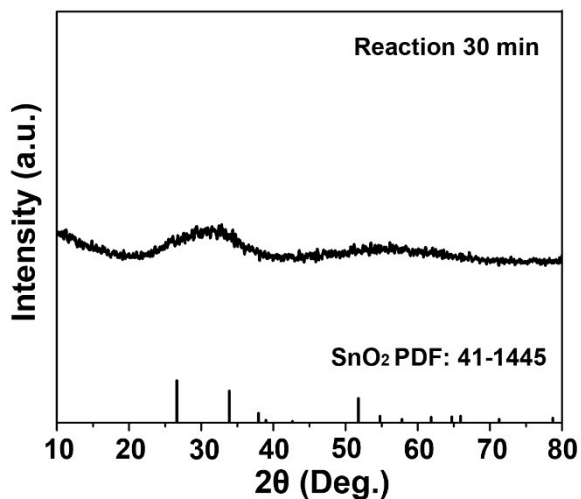


Fig. S2. XRD pattern of the precursor after heating for 30 min.

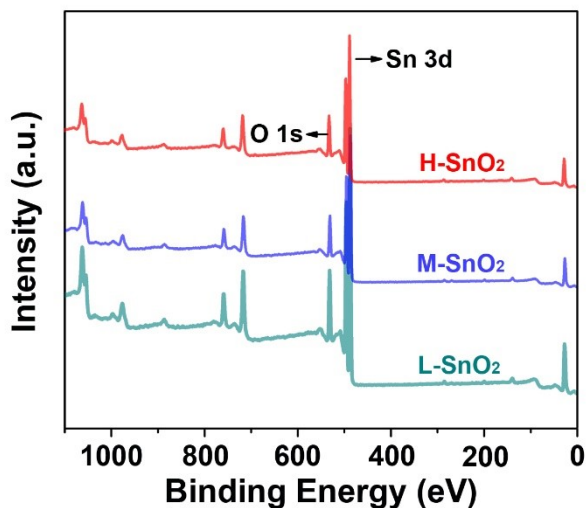


Fig. S3. XPS overall survey spectra of the H-SnO₂, M-SnO₂ and L-SnO₂.

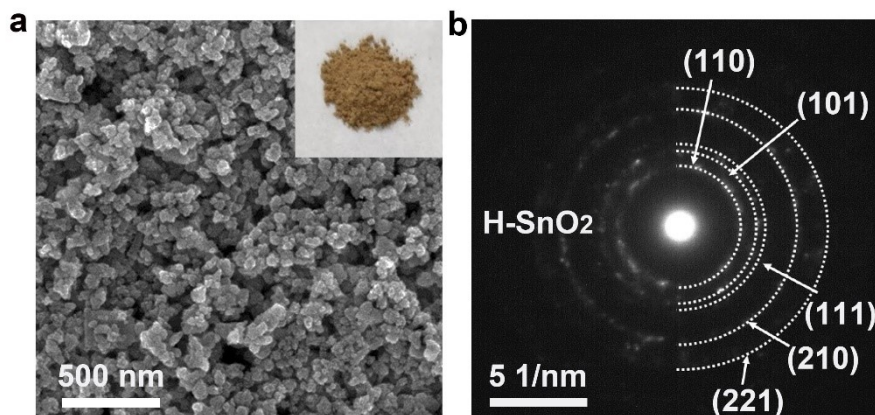


Fig. S4. (a) SEM image (inset showing the DigiPhoto image), (b) SAED pattern of the H-SnO₂.

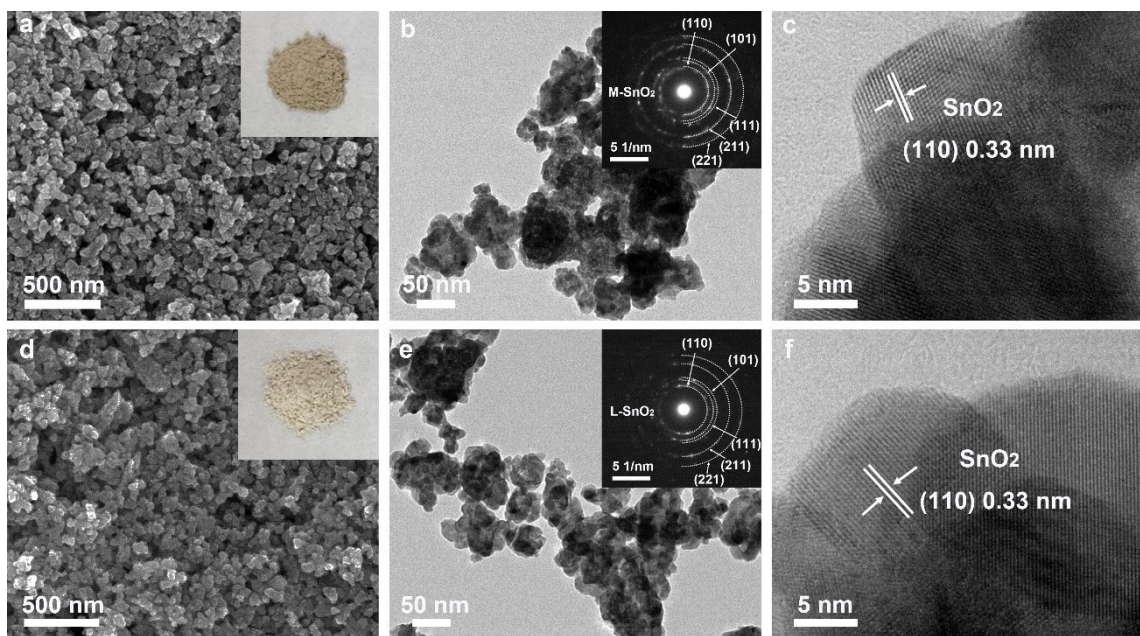


Fig. S5. (a, d) SEM images (inset showing the DigiPhoto images), (b, e) low-magnification TEM images and the corresponding SAED pattern, (c, f) high-magnification TEM images of M-SnO₂ and L-SnO₂, respectively.

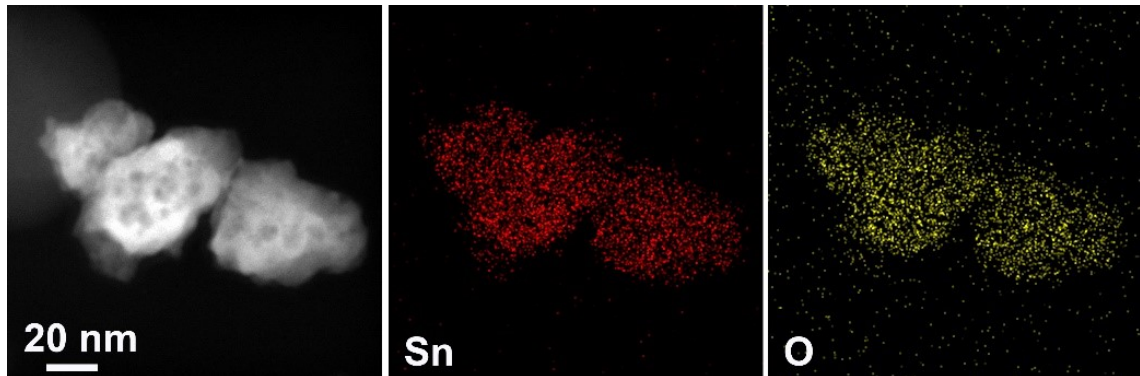


Fig. S6. TEM-EDS mapping of Sn, O of the H-SnO₂.

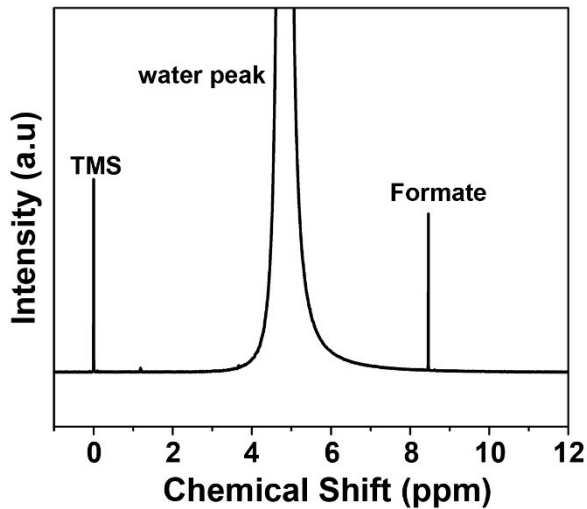


Fig. S7. ¹H NMR of liquid products.

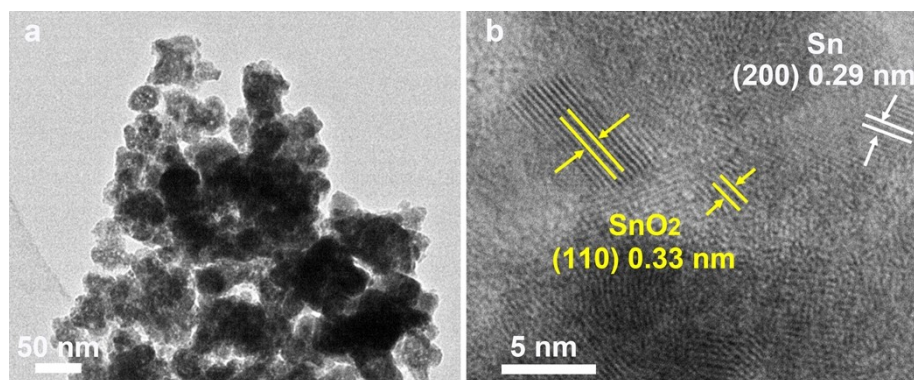


Fig. S8. (a, b) Low-magnification and high-magnification TEM images of the H-SnO₂ after long-term stability at -0.9 V vs. RHE.

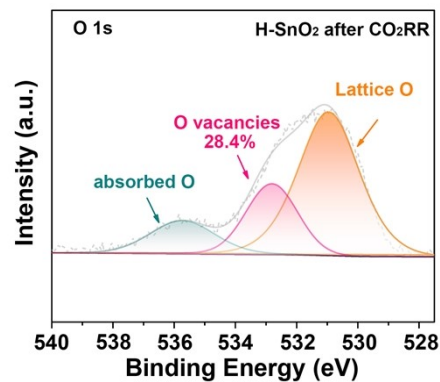


Fig. S9. O 1s XPS spectrum for the H-SnO₂ after long-term stability at -0.9 V vs. RHE.

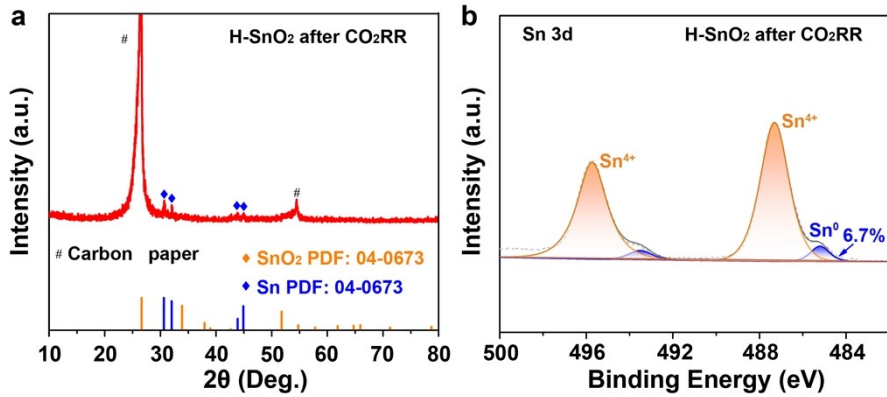


Fig. S10. (a) XRD pattern and (b) Sn 3d XPS spectrum for the H-SnO₂ after long-term stability at -0.9 V vs. RHE.

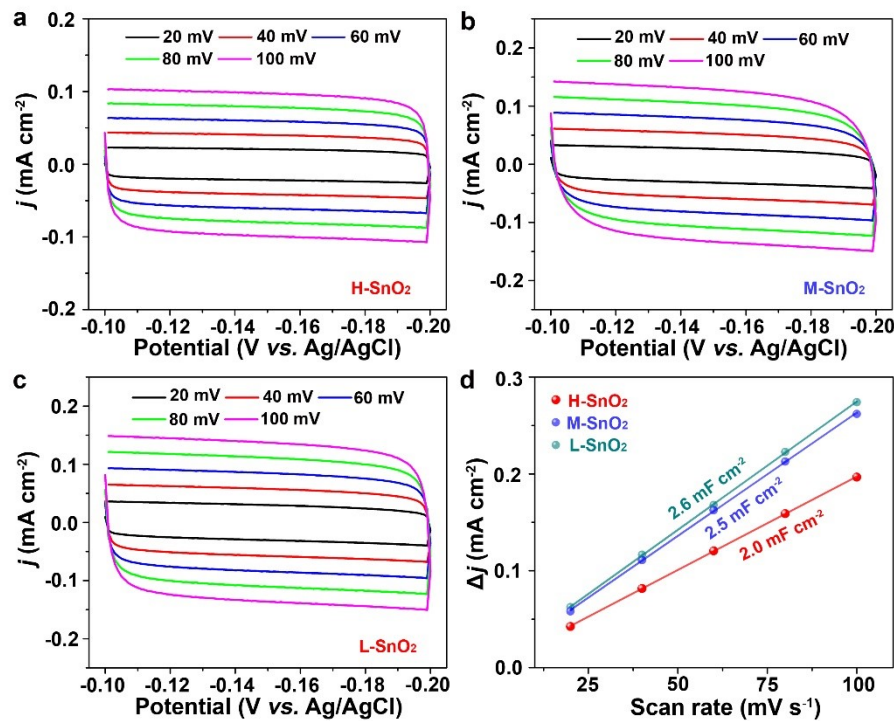


Fig. S11. CV curves of (a) the H-SnO₂, (b) M-SnO₂ and (c) L-SnO₂, respectively, (d) electrochemical double-layer capacitance (C_{dl}) of the H-SnO₂, M-SnO₂ and L-SnO₂.

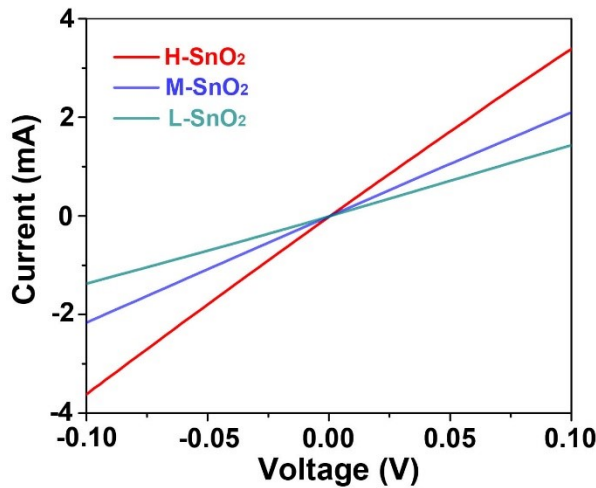


Fig. S12. I-V curves of the H-SnO₂, M-SnO₂, L-SnO₂.

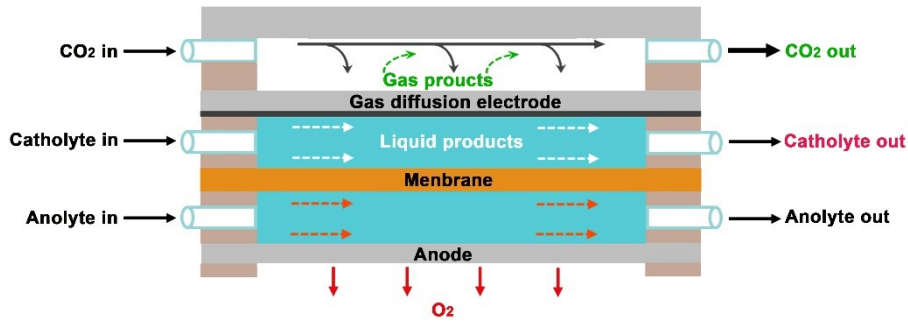


Fig. S13. The schematic diagram of the self-designed flow cell.

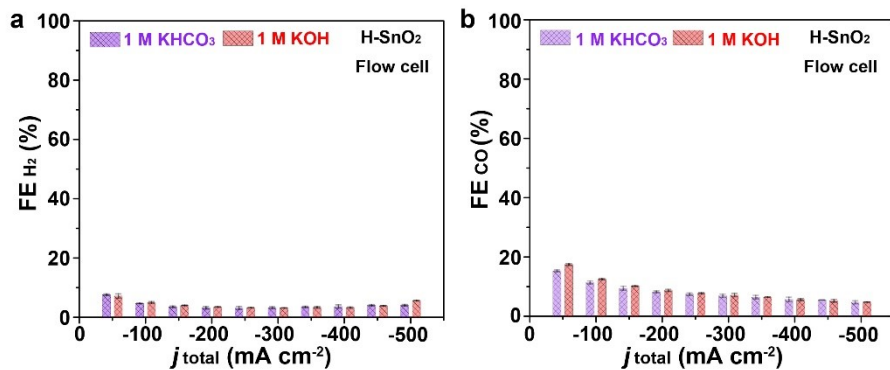


Fig. S14. (a) FE of generating H₂, (b) FE of generating CO on the H-SnO₂ at different applied currents in a flow cell filled with 1 M KOH or 1 M KHCO₃ electrolyte.

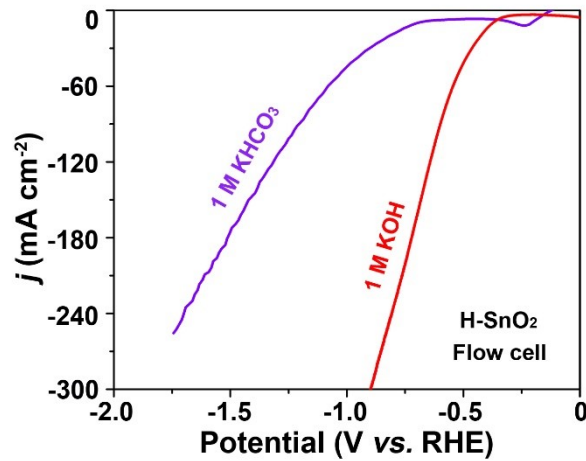


Fig. S15. Polarization curves of the H-SnO₂ in a flow cell filled with 1 M KOH or 1 M KHCO₃ electrolyte.

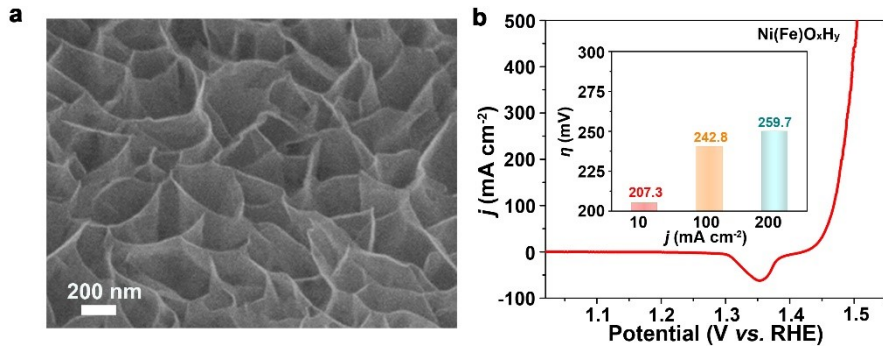


Fig. S16. (a)The SEM image of the Ni(Fe)O_xH_y nanosheets array on Ni foam, (b) OER polarization curve and overpotential (η) at 10, 100 and 200 mA cm^{-2} of the Ni(Fe)O_xH_y sample in 1 M KOH.

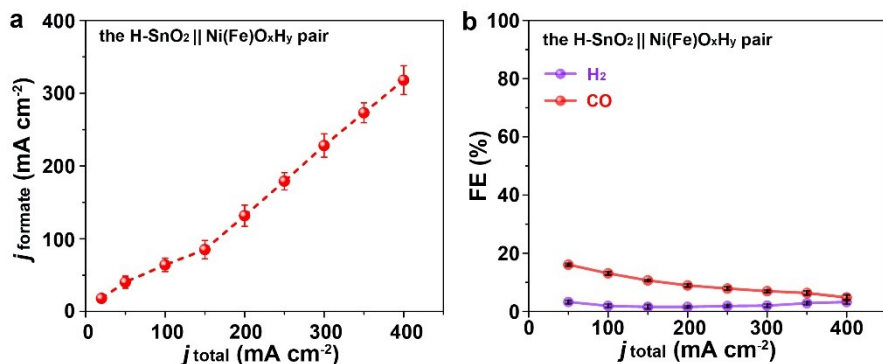


Fig. S17. (a) j_{formate} , (b) the FE_{H_2} and FE_{CO} at different applied currents using a two-electrode CO₂RR-OER full cell based on the H-SnO₂||Ni(Fe)O_xH_y pair filled with 1 M KOH electrolyte.

Supporting Tables

Table S1. CO₂RR performance comparison of Sn-based electrocatalysts for formate production by CO₂RR in an H-type cell.

Catalyst	Electrolyte	Potential (V)	j_{formate} (mA cm ⁻²)	FE _{formate} (%)	Ref.
SnO ₂ -CNT	0.5 M KHCO ₃	-0.92	10.9	76.3	1
SnO ₂	0.1 M KHCO ₃	-1.25	17.2	83.2	2
mSnO ₂ NTs	0.5 M KHCO ₃	-1.10	5.6	83.5	3
SnO ₂ QWs	0.1 M KHCO ₃	-0.95	7.2	79.0	4
V _o -N-SnO ₂ NS	0.1 M NaHCO ₃	-0.90	6.9	81.6	5
SnO ₂ /OC	0.1 M KHCO ₃	-0.90	5.0	0.1	6
SnO ₂ -V _o @N-C	0.1 M KHCO ₃	-0.95	5.6	70.2	7
H-SnO ₂	0.5 M KHCO ₃	-0.90	16.6	82.8	This work

Table S2 The fitting results of Nyquist plots of the three SnO₂ samples with different O_v concentrations at -0.9 V vs. RHE.

Catalyst	R_s (Ω)	R_{ct} (Ω)	C_{dl} (F)
H-SnO ₂	3.62	11.80	0.88
M-SnO ₂	4.26	15.50	0.83
L-SnO ₂	3.88	18.80	0.88

Table S3. CO₂RR performance comparison of metal-based electrocatalysts for formate production by CO₂RR in a flow cell.

Catalyst	Electrolyte	j_{formate} range (mA cm ⁻²) over 80% and the corresponding potential range	Max- j_{formate} (mA cm ⁻²)	Ref.
Bi nanosheet derived from BiOBr	2 M KHCO ₃	~90.0 and ~180.0 (-0.70 and -0.80 V)	~180.0	8
Atomically thin bismuthene	1 M KOH	99.8 to 198.4 (-0.57 to -0.75 V)	198.4	9
Bi oxide nanotubes	1.0 M KOH	~100.0 to 205.8 (-0.52 to -0.58 V)	205.8	10
Bi ₂ O ₃ @C	1.0 M KOH	~25.0 to 208.0 (-0.50 to -1.10)	208.0	11
Bi@Sn core-shell	2.0 M KHCO ₃	~22.5 to ~225.0 (-0.80 to -1.15)	250.0	12
Bismuthene nanosheets	1.0 M KHCO ₃	~10.0 to ~270.0 (-0.64 to -1.40)	280.0	13
Sn _{0.80} Bi _{0.20} @ Bi-SnO _x	0.5 M KHCO ₃	~5.0 to ~22.5 (-0.68 to -1.98)	75.0	14
Sn _{2.7} Cu	1.0 M KOH	~10.0 to ~375.5 (-0.32 to -0.7)	375.0	15
Sn	2.0 M KHCO ₃	~22.7 to ~226.3 (-0.32 to -0.7)	226.3	16

H-SnO ₂	1 M KHCO ₃	40.4 to 466.2 (-1.06 to -2.17)	466.2	This work
H-SnO ₂	1 M KOH	82.5 to 447.6 (-0.58 to -1.17)	447.6	This work

Table S4. Comparison of the maximum full-cell energy efficiencies of electrocatalysts for CO₂RR in a flow cell type.

Cathode	Anode	Electrolyte	Max-EE	Product	Ref.
B-doped Sn	IrO ₂	1 M KOH	50.0	formate	17
Sn nanoparticles	Pt	1 M KOH	64.7	formate	18
Au nanoparticles	IrO ₂	Alkaline polymer	~62.0	CO	19
Ag nanoparticles	IrO ₂	3 M KOH	~54.0	CO	20
C-Bi RDs	IrO ₂	1 M KOH	69.5	formate	21
Pb nanoparticles	PtRu	0.5 M K ₂ SO ₄	~49.0	CO	22
Ag nanoparticles	IrO ₂	1.5 M KHCO ₃	47.0	CO	23
H-SnO ₂	Ni(Fe)O _x H _y	1 M KOH	54.9	formate	This work

References

- [1] K. Pavithra, S. M. S. Kumar, *Catal. Sci. Technol.*, 2020, **10**, 1311-1322.
- [2] H. Liu, Y. Q. Su, S.Y. Kuang, E. Hensen, S. Zhang, X. B. Ma, *J. Mater. Chem. A*, 2019, **9**, 7848-7856.

- [3] F. C. Wei, T. T. Wang, X. L. Jiang, Y. Ai, A. Y. Cui, J. Cui, J. W. Fu, J. G. Cheng, L. C. Lei, Y. Hou, S. H. Liu, *Adv. Funct. Mater.*, 2020, **30**, 2002092.
- [4] S. B. Liu, J. Xiao, X. F. Lu, J. Wang, X. Wang, X. W. Lou, *Angew. Chem. Int. Ed.*, 2019, **58**, 8499-8503.
- [5] Z. J. Li, A. Cao, Q. Zheng, Y. Y. Fu, T. T. Wang, K. T. Arul, J. L. Chen, B. Yang, N. D. Mohd Adli, L. C. Lei, C. L. Dong, J. P. Xiao, G. Wu, Y. Hou, *Adv. Mater.*, 2021, **33**, 2005113.
- [6] Z. Y. Kuang, W. P. Zhao, C. L. Peng, Q. M. Zhang, Y. Xue, Z. X. Li, H. L. Yao, X. X. Zhou, H. R. Chen, *ChemSusChem*, 2020, **13**, 5896-5900.
- [7] Y. S. Yuan, K. Sheng, G. L. Zhuang, Q. Y. Li, C. Dou, Q. J. Fang, W. W. Zhan, H. Gao, D. Sun, X. G. Han, *Chem. Commun.*, 2021, **57**, 8636-8639.
- [8] F. P. Garcia de Arquer, O.S. Bushuyev, P. De Luna, C.T. Dinh, A. Seifitokaldani, M.I. Saidaminov, C.S. Tan, L.N. Quan, A. Proppe, M.G. Kibria, S.O. Kelley, D. Sinton, E.H. Sargent, *Adv. Mater.*, 2018, **30**, 1802858.
- [9] C. S. Cao, D. D. Ma, J. F. Gu, X. Y. Xie, G. Zeng, X. F. Li, S. G. Han, Q. L. Zhu, X. T. Wu, Q. Xu, *Angew. Chem. Int. Ed.*, 2020, **59**, 15014-15020.
- [10] Q. F. Gong, P. Ding, M. Q. Xu, X. R. Zhu, M. Y. Wang, J. Deng, Q. Ma, N. Han, Y. Zhu, J. Lu, Z. X. Feng, Y. f. Li. W. Zhou, Y. G. Li, *Nat. Commun.*, 2019, **10**, 2807.
- [11] P. L. Deng, F. Yang, Z. T. Wang, S. H. Chen, Y. Z. Zhou, S. H. Zaman, B. Y. Xia, *Angew. Chem. Int. Ed.*, 2020, **59**, 10807-10813.
- [12] Y. L. Xing, X. D. Kong, X. Guo, Y. Liu, Q. Y. Li, Y. Z. Zhang, Y. L. Sheng, X. P. Yang, Z. G. Geng, J. Zeng, *Adv. Sci.*, 2020, **7**, 1902989.
- [13] W. X. Ma, J. Bu, Z. P. Liu, C. Yan, Y. Yao, N. H. Chang, H. P. Zhang, T. Wang, J. Zhang, *Adv. Funct. Mater.*, 2020, **31**, 2006704.
- [14] Q. Yang, Q. L. Wu, Y. Liu, S. P. Luo, X. T. Wu, X. X. Zhao, H. Y. Zou, B. H. Long, W. Chen, Y. J. Liao, L. X. Li, P. K. Shen, L. L. Duan, Z. W. Quan, *Adv. Mater.*, 2020, **32**, 2002822.

- [15] K. Ye, Z. W. Zhou, J. Q. Shao, L. Lin, D. F. Gao, N. Ta, R. Si, G. X. Wang, X. H. Bao, *Angew. Chem. Int. Ed.*, 2020, **59**, 4814-4821.
- [16] Y. L. Xing, X. D. Kong, X. Guo, Y. Liu, Q. Y. Li, Y. Z. Zhang, Y. L. Sheng, X. P. Yang, Z. G. Geng, J. Zeng, *Adv. Sci.*, 2020, **7**, 1902989.
- [17] Z. Y. Li, T. Y. Zhang, R.M. Yadav, J. F. Zhang, J. J. Wu, *J. Electrochem. Soc.*, 2020, **167**, 114508.
- [18] W. Lee, Y.E. Kim, M.H. Youn, S.K. Jeong, K.T. Park, *Angew. Chem. Int. Ed.*, 2018, **57**, 6883-6887.
- [19] Z. L. Yin, H. Q. Peng, X. Wei, H. Zhou, J. Gong, M. M. Huai, L. Xiao, G. W. Wang, J. T. Lu, L. Zhuang, *Energy Environ. Sci.*, 2019, **12**, 2455.
- [20] S. Verma, X. Lu, S. Ma, R.I. Masel, P.J.A. Kenis, *Phys. Chem. Chem. Phys.*, 2016, **18**, 7075.
- [21] H. Xie, T. Zhang, R. K. Xie, Z. F. Hou, X. C. Ji, Y. Y. Pang, S. Q. Chen, M. Titirici, H. M. Weng, G. L. Chai, *Adv. Mater.*, 2021, **33**, 2008373.
- [22] X. X. Lu, D. Leung, H. Z. Wang, J. Xuan, *Appl. Energy*, 2017, **194**, 549-559.
- [23] T. Haas, R. Krause, R. Weber, M. Demler, G. Schmid, *Nat. Catal.*, 2018, **1**, 32-39.